Pergamon

www.elsevier.com/locate/jaerosci

PII: S0021-8502(99)00055-5

J. Aerosol Sci. Vol. 31, No. 3, pp. 293–305, 2000

Printed in Great Britain
0021-8502/00/$ - see front matter

ON THE EFFECTS OF ELECTROHYDRODYNAMIC FLOWS AND TURBULENCE ON AEROSOL TRANSPORT AND COLLECTION IN WIRE-PLATE ELECTROSTATIC PRECIPITATORS

Alfredo Soldati*

Centro di Fluidodinamica e Idraulica and Dipartimento di Scienze e Tecnologie, Chimiche Università di Udine, 33100, Udine, Italy

(*First received* 7 *January* 1999; *and in final form* 29 *April* 1999)

Abstract—Predicting transport of aerosols or particles in wire-plate electrostatic precipitators is complicated by the influence of EHD flows and turbulent flow field. In this work we use the direct numerical simulation by Soldati and Banerjee (1998) to analyze the effects of the EHD flows and of turbulence on particle transport and collection efficiency. Particles of different size and charge were tracked in two different flow fields corresponding to different potential applied to the wires of the precipitator. Results were compared against simulations in which the electrostatic field acted only on particles, − i.e. no EHD flows. It is apparent that EHD flows are large advective motions with scale of the wire-to-wall distance and have a strong effect on the local behavior of particles, sweeping them into different regions of the channel. However, it was found that the overall collection efficiency of the precipitator is not significantly affected by the presence of EHD flows. Even in the vicinity of the wall, EHD flows appear to have negligible influence on particle deposition. © 2000 Elsevier Science Ltd. All rights reserved

1. INTRODUCTION

Electrostatic precipitators (ESP) are designed to purify gas streams from airborne particles or aerosols of micrometric size: a charge is placed on the particles to be driven toward collecting electrodes by the applied electrostatic field. More stringent regulations on pollutant emission require optimization of the design criteria employed for ESPs. The efficiency of ESPs depends on the transport characteristics of airborne particles, knowledge of which is therefore fundamental for proper design, and on other different effects as by-pass flows, back-corona and particle re-entrainment mechanisms among others. In industrial applications—e.g. purification of waste gases from coal burning plants, or from cement production plants, among others—the most commonly used ESPs are the wire-plate type, a schematic of which is shown in Fig. 1. In this configuration, the wires are kept at a potential high enough, first, to discharge the ionic species required to charge the initially neutral airborne particles, and, second, to generate the electrostatic force required to drive the charged particles toward the collecting plates. However, the dispersed ions which are driven toward the walls by the Coulomb force, collide with fluid molecules and transfer momentum to them. In this way, fluid motions of electrohydrodynamic (EHD) origin are generated. Under conditions of uniform discharge from the wires, the EHD flows take the form of large, spanwise, counter-rotating vortical flows with a scale equal to the wire-to-wall distance. The effects of EHD flows on the fluid mechanics and on particle transport in a wire-plate ESP have long been debated (Leonard *et al*., 1980; Cooperman, 1982; Leonard *et al*., 1983; Atten *et al*., 1987; Koopmans, 1988; Davidson and McKinney, 1991, to cite a few), but so far no definite conclusion has been reached. Even though other effects may be of importance, optimal ESP design requires accurate prediction of particle collection at the wall which, in turn, requires accurate evaluation of fluid mechanics and particle transport

* E-mail: alfredo@euterpe.dstc.uniud.it

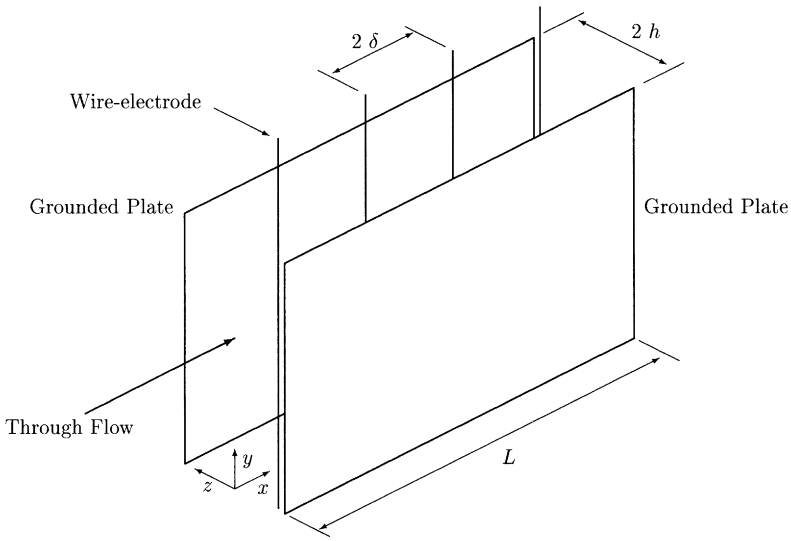

Wire to Wire Spacing	$2\delta = 0.0628\ m$	Wire Length	$l = 0.125\ m$
Duct Width	$2\ h = 0.04\ m$	Fluid Density	$\rho = 1.38\ kg/m^3$
Duct Length	$L = 0.25\ m$	Fluid Viscosity	$\nu = 1.66 \cdot 10^{-5}\ m^2/s$

Fig. 1. Schematic of wire-plate electrostatic precipitator.

parameters. This means first, solving the problem of interactions of the EHD flows with the turbulent flow field correctly, and, second, describing turbulent particle transport.

Turbulent transport has generally been overlooked and common industrial approaches are limited to correlations still based on the oversimplified theory of Deutsch (1922), based on the assumption that turbulent dispersion is infinite. Other approaches (Williams and Jackson, 1962; Leonard *et al.*, 1980), are based on the use of a two-dimensional, lumped parameter advection–diffusion equation (ADE) with transport coefficients determined *a posteriori.*

Characterizing EHD flows in the turbulent through flow of a wire-plate ESP has been the object of a number of experimental (see Leonard *et al.*, 1983; Davidson and McKinney, 1991; Kallio and Stock, 1992, among others) and numerical works (Bernstein and Crowe, 1981; Kallio and Stock, 1992; Soldati and Banerjee, 1998). Experimental analysis is difficult because of the presence of the electrostatic field, which influences measurements of laser doppler anemometers and hot-wire probes. Numerical analyses have been performed by k–ε models for turbulence (Bernstein and Crowe, 1981; Kallio and Stock, 1992), which are inadequate to capture turbulence features and complex energy transfer between EHD vortical flows and turbulence field. In our recent paper (Soldati and Banerjee, 1998), we used a direct numerical simulation (DNS) to analyze the turbulent flow field in an ESP including the effects of EHD flows.

Recently, Lagrangian simulations of particle transport in wire-plate ESP were performed by several researchers (Choi and Fletcher, 1997, 1998; Gallimberti, 1998, among others). These simulations are based on particle tracking in the flow field calculated by a finite-volume solver of the Navier–Stokes equations including a turbulence k–ε model and the influence of EHD flows. However, these analyses can give the overall characteristics of particle transport at most and do not allow a deeper investigation.

The object of the present work is to evaluate the influence of the EHD flows on particle transport and on ESP collection efficiency by means of particle tracking in the flow field obtained by direct numerical simulation. It is generally believed that these flow structures reduce the efficiency of ESPs (Davidson and McKinney, 1991) by increasing turbulent dispersion mechanisms. We performed Lagrangian simulations by dispersing swarms of precharged particles in the flow field of a wire-plate precipitator including the EHD flows.

We also performed simulations in which the electrostatic force was acting only on the precharged particles without affecting the flow field. Results seem to indicate that EHD flows have negligible influence on particle overall collection and on particle deposition at the wall.

2. METHODOLOGY

2.1. *Flow field*

To describe the flow field of a wire-plate ESP, the following momentum balance equations must be solved:

$$\rho\left[\frac{\partial u_i}{\partial t}+u_j\frac{\partial u_i}{\partial x_j}\right]=-\frac{\partial \mathscr{P}}{\partial x_i}+\mu\frac{\partial^2 u_i}{\partial x_j\partial x_j}+F_i, \tag{1}$$

where u_i are the dimensional velocity components along the three directions x_i (with x_1 being the streamwise, x_2 being the spanwise and x_3 being the wall-normal directions), $\mathscr{P}$ is pressure, ρ and μ are fluid density and dynamic viscosity, respectively, and F_i are the components of the electrostatic body force. Since the pressure gradient was maintained constant for the simulations, the shear Reynolds number was equal to 108 for all the simulations we performed and equal to a previous DNS of turbulent channel flow without EHD effects performed by Soldati *et al.* (1993). Simulations presented here were run with $128\times64\times65$ nodes in a box of dimensionless size $1357\times678\times216$ in wall units (dimensionless variables in wall units are indicated by the superscript $+$) and a timestep $\Delta t^+=0.038$. This gives a resolution of $\Delta x_1^+=10.6$, $\Delta x_2^+=10.6$, and Δx_3^+ ranging from 0.13 next to the walls to 5.3 in the center of the channel. For both cases, simulations were started from the steady turbulent channel flow computed in Soldati *et al.* (1993) by turning on the electrostatic body force.

For the case under consideration, which may represent positive discharge, the body force depends only on x and z, implying that the body force distribution does not fluctuate because of ionic convection. This is a realistic assumption, since ions have a drift velocity of about $100\ \mathrm{m\,s^{-1}}$ in air while the mean flow velocity is about $1\ \mathrm{m\,s^{-1}}$. Here the coupling is "one-way", i.e. the fluid does not modify the electrostatic body forces, which is calculated from the following set of equations:

$$\frac{\partial^2 V}{\partial x_i^2}=-\frac{\rho_c}{\varepsilon_0}, \tag{2}$$

$$\rho_c^2=\varepsilon_0\frac{\partial\rho_c}{\partial x_i}\frac{\partial V}{\partial x_i}=-\varepsilon_0\frac{\partial\rho_c}{\partial x_i}E_i, \tag{3}$$

$$E_i=-\frac{\partial V}{\partial x_i}, \tag{4}$$

$$J_i=-\rho_c\beta E_i, \tag{5}$$

where ε_0 is air permittivity ($\varepsilon_0=8.854\times10^{-12}$) and $\beta=1.4311\times10^{-4}\ \mathrm{m^2/V\,s}$ is ionic mobility (McDaniel and Mason, 1973, Lai *et al.*, 1995) for positive discharge in air. These equations were solved by a two dimensional, finite-difference scheme (Leutert and Bohlen, 1972). Briefly, this scheme is based on an initial guess for the space-charge density at the wire followed by iterative solution of equations (2) and (3) until convergence of the plate current density is obtained.

Two different simulations were run for two different distributions of the body force corresponding to potentials of 32 000 and 42 000 V applied to the wires. In the low-voltage case, the linear current density at the plate was $I_1=0.3\times10^{-3}$ A/m, whereas in the high-voltage case it was $I_2=0.75\times10^{-3}$ A/m.

Distribution of the body force in the x–z section (streamwise and wall-normal) for a portion of the domain comprising two wires can be examined in Fig. 2a. If such a body

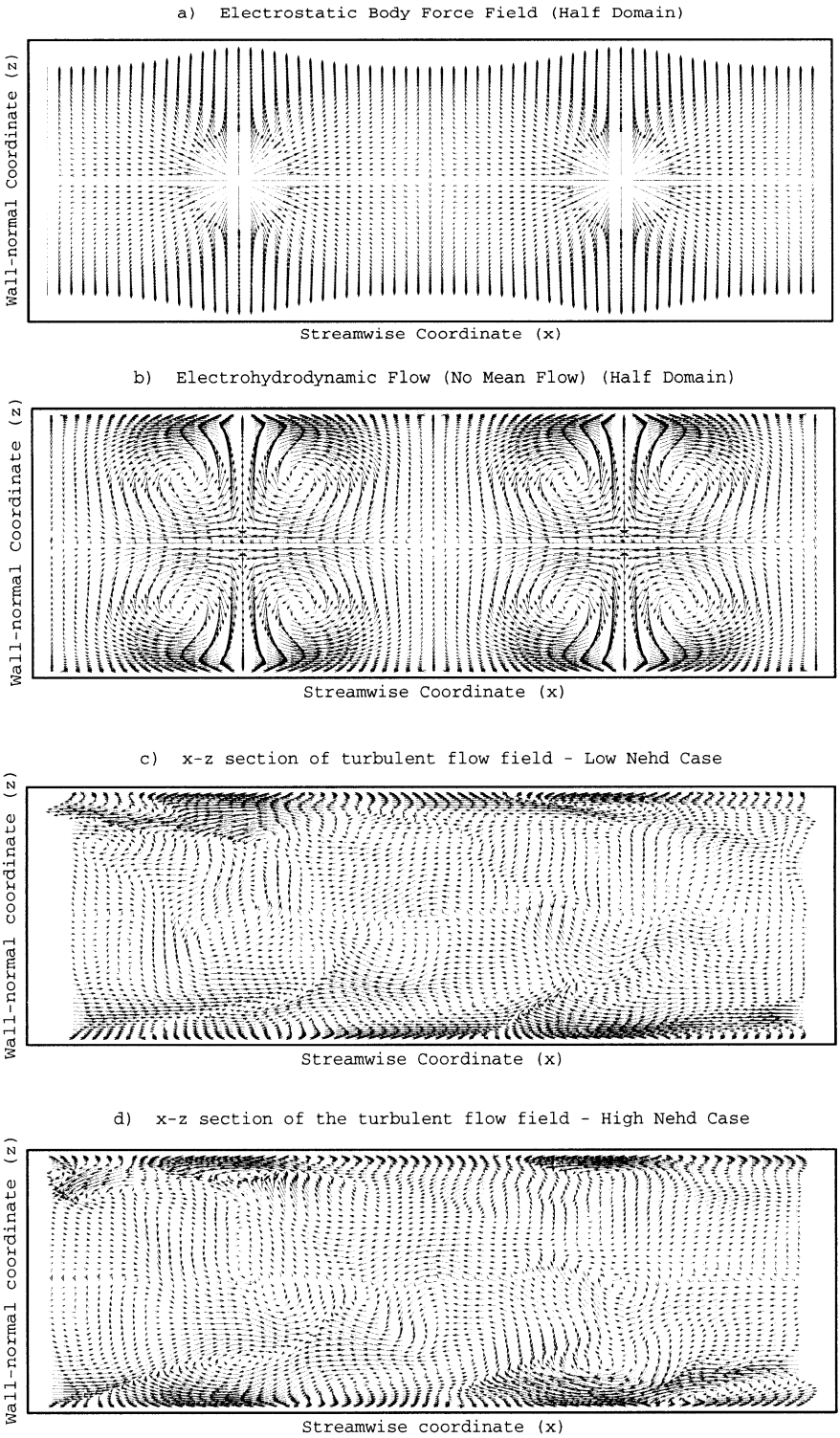

Fig. 2. Electrostatic body force and Flow field. From top to bottom: (a) Distribution of EHD body force; (b) Structure of EHD flows in still fluid; (c) Structure of EHD flows in turbulent through flow at low intensity of electrostatic field; (d) structure of EHD flows in turbulent through flow at high intensity of electrostatic field.

force distribution is applied to still fluid, a regular array of EHD structures appears as shown in Fig. 2b. When a pressure gradient is imposed on the fluid and the flow is turbulent, the non-linear interactions between EHD structures and turbulence field modify the

scenario and the instantaneous, fluctuating flow field shown in Fig. 2c and Fig. 2d is obtained for the low- and high-voltage cases, respectively. A detailed description of statistics and instantaneous features of the flow field was reported previously (Soldati and Banerjee, 1998).

One significant result was that the superposition of the EHD flows onto the turbulent channel flow implies a significant modification of turbulence structure in the wall region. In particular, changes in turbulent transfer mechanisms were observed. This leads to drag reduction by modifying turbulent transfer mechanisms and it is expected the changes will play a role in the local behavior of particles to be separated by an ESP. These analyses will be presented elsewhere (Soldati, 1999).

In simulations with both low and high voltage, drag reduction was observed. Since the simulations were performed for the same pressure gradient, mean velocity increased with respect to a previous channel flow simulation calculated for the same pressure gradient (Soldati *et al*., 1993). Considering air (kinematic viscosity $\nu = 16.6 \times 10^{-6}\,\mathrm{m^2\,s^{-1}}$), and a duct width of $2h = 0.04\ m$, the mean velocity in the previous channel flow simulation was $1.16\,\mathrm{m\,s^{-1}}$, but, in the new low-voltage case, it was $1.19\,\mathrm{m\,s^{-1}}$ ($\sim 3\%$ larger) and in the high-voltage case, it was $1.23\,\mathrm{m\,s^{-1}}$ ($\sim 6\%$ larger). All of the simulations used in this work can be characterized by Reynolds number based on mean velocity and duct width, which is ~ 2795 in the channel flow case, ~ 2857 in the low voltage case, and ~ 2964 in the high-voltage case, and by EHD number, N_{EHD}. This dimensionless number represents the ratio between the electrostatic body force and inertial forces acting on a fluid parcel. In Leonard *et al*. (1983), and in this paper,

$$N_{\mathrm{EHD}} = \frac{i}{l\rho\beta U^2}, \tag{6}$$

where i represents the total current at the plate, l the length of the wire, ρ the fluid density, and U the mean flow velocity. In the limiting case of $N_{\mathrm{EHD}} = 0$, the flow is unaffected by electrohydrodynamic forces (i.e. it is plane Poiseuille flow). In the limiting case $N_{\mathrm{EHD}} = \infty$, the through-flow does not affect EHD flows, as shown in Fig. 2b. The actual value of the N_{EHD} number is 1.1 in the low-intensity case and 2.5 in the high intensity case.

2.2. *Particle tracking*

Airborne particles to be collected are subject to the combined effects of the flow field, the electrostatic body force, and gravity. The procedure employed in this work is the same as in Soldati *et al*. (1993, 1997): we shall describe it briefly. The vectorial equation of motion is

$$\frac{\mathrm{d}\mathbf{v}}{\mathrm{d}t} = -\frac{\mathbf{v}-\mathbf{u}}{\tau_{\mathrm{p}}} f(\mathrm{Re_p}) + \frac{\rho - \rho_{\mathrm{p}}}{\rho_{\mathrm{p}}}\,\mathbf{g} + \frac{1}{\mathrm{Fr_p^2}}\,\mathbf{e}, \tag{7}$$

where, $\mathbf{v}$ is particle velocity, $\mathbf{g}$ is the gravity vector, $\mathbf{e}$ is the electric field unit vector and τ_{p} is the relaxation time (the Stokesian response time), defined as

$$\tau_{\mathrm{p}} = \frac{d_{\mathrm{p}}^2 \rho_{\mathrm{p}}}{18\mu}, \tag{8}$$

where ρ_{p} is particle density, μ is fluid viscosity and Fr_{p} is the dimensionless electric-Froude number (Soldati *et al*., 1995), defined as

$$\mathrm{Fr_p} = \sqrt{\frac{m_{\mathrm{p}}}{q_{\mathrm{p}}\bar{E}}}, \tag{9}$$

in which m_{p} is particle mass, $\bar{E}$ is the intensity of the average electrostatic field and q_{p} is particle charge. In presence of a distributed space charge, particle charging would depend on the local value of the space charge. Since this would introduce a further complicative effect in the analysis of the results, we considered the transport of precharged particles. In presence of free ions, the charge of a particle is a function of the applied electrostatic field via

the equation

$$q_p = 3\pi \frac{\varepsilon}{\varepsilon + 2} \varepsilon_0 \bar{E}_c d_p^2, \tag{10}$$

where ε_0 is the permittivity of vacuum, $\bar{E}_c$ is the value of the electrostatic field using for precharging the aerosol particles, and ε is the dielectric constant of the particle, which for the present work was taken to be equal to 2, simulating an aerosol of oleic acid (Leonard *et al*., 1982; Kihm, 1987). With the aim of investigating on particle transport, we should ensure that particle charge is the same in the whole domain not being a function of the local electrostatic field. To ensure this, particle precharge should be higher than the maximum charge a particle could acquire when exposed to the ionic space charge. In previous experimental works (Kihm, 1987; Self *et al*., 1987) precharge approximately three times larger than the maximum particle charge the ionic discharge could produce was used. However, for the values of electrostatic body force used in these simulations, this would produce a very large electric migration velocity of particles, which thus would be collected very rapidly. Therefore, we assumed that particles enter the precipitator precharged and that their charge remains the same along their trajectory. In the high-intensity case, we considered an uniform charging field of $\bar{E}_c = 224.7\ \mathrm{kV\,m^{-1}}$, whereas in the low-intensity case it was $\bar{E}_c = 164.8\ \mathrm{kV\,m^{-1}}$.

In equation (7), $f(\mathrm{Re_p})$ is a function of the particle Reynolds number, $\mathrm{Re_p}$, which depends on the fluid dynamic drag law adopted. In this work, we used the form proposed by Rowe and Henwood (1962), i.e.

$$f(\mathrm{Re_p}) = 1 + 0.15\mathrm{Re_p}^{0.687}. \tag{11}$$

The trajectory of each particle was calculated by integration of equation (7) performed by an explicit method. The velocity of the fluid at each particle position was calculated directly from the triple sums of the spectral coefficients. This method is accurate but its cost in terms of computer time rapidly becomes prohibitive with the number of particles tracked (Yeung and Pope, 1988). For the number of particles used in present simulations (4000), the computer time is comparable to that required for other types of interpolations. The initial velocities of the particles were set equal to the fluid velocity at each particle location (see Soldati *et al*., 1997 for a discussion). The motion of particles can be characterized by the particle relaxation time, τ_p, which is an indicator of particle inertia, by the square of particle electrostatic Froude number, Fr_p^2, and finally by the free migration velocity, w_{St}, which is defined as

$$w_{St} = \frac{q_p \bar{E}}{3\pi d_p \mu}. \tag{12}$$

Free migration velocity is calculated from the steady force balance on the particle in the Stokes regime and is the maximum velocity attainable by a particle subject to the average electrostatic field $\bar{E}$. This velocity is usually taken as representative of particle migration

Table 1. Parameters for particle transport simulation

d_p ($m \times 10^{-6}$)	τ_p (s)	ΔV(kV)	$\bar{E}$ (kV/m)	$q(C \times 10^{-16})$	w_{st}(cm/s)	$\mathrm{Fr_p}$
4	3.9×10^{-5}	42	380	1.5	7.67	0.15
		32	290	1.1	4.18	0.20
8	1.6×10^{-4}	42	380	6.0	15.1	0.21
		32	290	4.4	8.40	0.29
16	6.3×10^{-4}	42	380	24.0	30.3	0.30
		32	290	17.0	16.7	0.41
32	2.5×10^{-3}	42	380	97.0	60.6	0.43
		32	290	70.0	33.4	0.57

Data have been calculated for particles with dielectric constant $\varepsilon = 2$. Charging field was uniform and equal to $\bar{E}_c = 224.7$ kV/m in the high intensity case, and to $\bar{E}_c = 164.8$ kV/m in the low intensity case. $\bar{E}$ is the average value of the electrostatic field in the precipitator.

velocity toward the collecting plate of a precipitator. In the present simulations, particles are assumed to be rigid and pointwise, and at a concentration low enough for particle–particle interaction due to either inertial force or electrostatic repulsion to be negligible. Dispersion of particles of different diameter—d_p equal to 4, 8, 16, 32 μm—in the range characteristic of ESP, was examined. Parameters characterizing the simulations are presented in Table 1. We simulated one dispersion of a swarm comprising 4000 particles, initially distributed uniformly throughout the whole channel, for both the low N_{EHD} and high N_{EHD} flow fields.

3. RESULTS OF DNS

3.1. *Effect of EHD flows and electrostatics on particle transport*

With regard to the electrostatic force distribution, shown in Fig. 2a, it can be observed that, when approaching the wires, entrained particles advected downstream have to *climb* against an adverse body force gradient whereas they *go down* the potential hill once they have passed the wires. Particles approaching the wires are thus slowed down by electrostatic body force and are then driven toward the walls. This effect is more pronounced the closer particles are to the channel centerline. In certain limiting cases, particles may be held in place for some time before being *kicked* toward the wall. Computer animations (Sisti, 1997) show clearly this effect, which is more pronounced for larger particles. A few snapshots of the position of particle swarms for 4 and 16 μm particles are shown in Fig. 3. Particles approaching the wires are slowed down by the electrostatic force and then they are swept toward the walls. However, since the electrostatic force rapidly decreases the greater the distance from the wire, particles can be re-entrained in the central region of the duct by turbulent diffusion mechanisms or by EHD flows. As expected, re-entrainment mechanisms are more effective for small particles, the motion of which is heavily affected by turbulent dispersion mechanisms. Larger particles can be transported back in the wire region only with difficulty and tend to be collected at the plate following preferential pathlines, as may be seen in Fig. 3.

The scales of the EHD flows are much too large, if compared to the scales of particle motion, to have a trapping effect on them by some segregation mechanism (Crowe *et al*., 1988; Brooke *et al*., 1992; Pedinotti *et al*., 1992, among others). Particles perceive the EHD flows as large, advective motions. However, EHD flows may have a local influence, sweeping particles into different regions of the channel. This observation was made already by Schmid and Umhauer (1996), who used a holographic technique to analyze particle behavior in presence of EHD flows in a wire-plate ESP.

The re-entrainment of small particles, which is an obstacle to high-collection efficiencies in ESP, may be observed in Fig. 4a and b, where the trajectory of some 4 μm particles is shown for the low and the high N_{EHD} case, respectively. Considering first Fig. 4b, the presence of the EHD backflows from the walls to the channel centerline can be clearly appreciated from the periodic trajectory of some particles. Observing, for instance, the trajectory with label *A*, it can be seen that the particle is pushed toward the wall by the electrostatic body force but, where the electrostatic force is weaker, in the middle of the wires, the EHD backflows sweep it toward the channel centerline. For other particles, such as the two labeled *B*, EHD flows contribute to push them toward the wall (see in particular the trajectory in proximity of the wall), with scarce re-entrainment effect. This effect is more pronounced in the high N_{EHD} case in which the intensity of the EHD flows is larger.

Going back to Fig. 3, we can see that regions with no particles appear immediately downstream the wires. This is because particles have to go around the potential hill and even if they are swept back into the central region by EHD flows, they are re-entrained immediately upstream the following wire. This effect is enhanced for increasing particle size and generates a large difference between the velocity of particles and fluid, as may be seen in Fig. 5, where mean flow velocity is compared against mean particle velocity averaged over the whole flow domain. As expected, the slip is larger for larger particles which tend to be

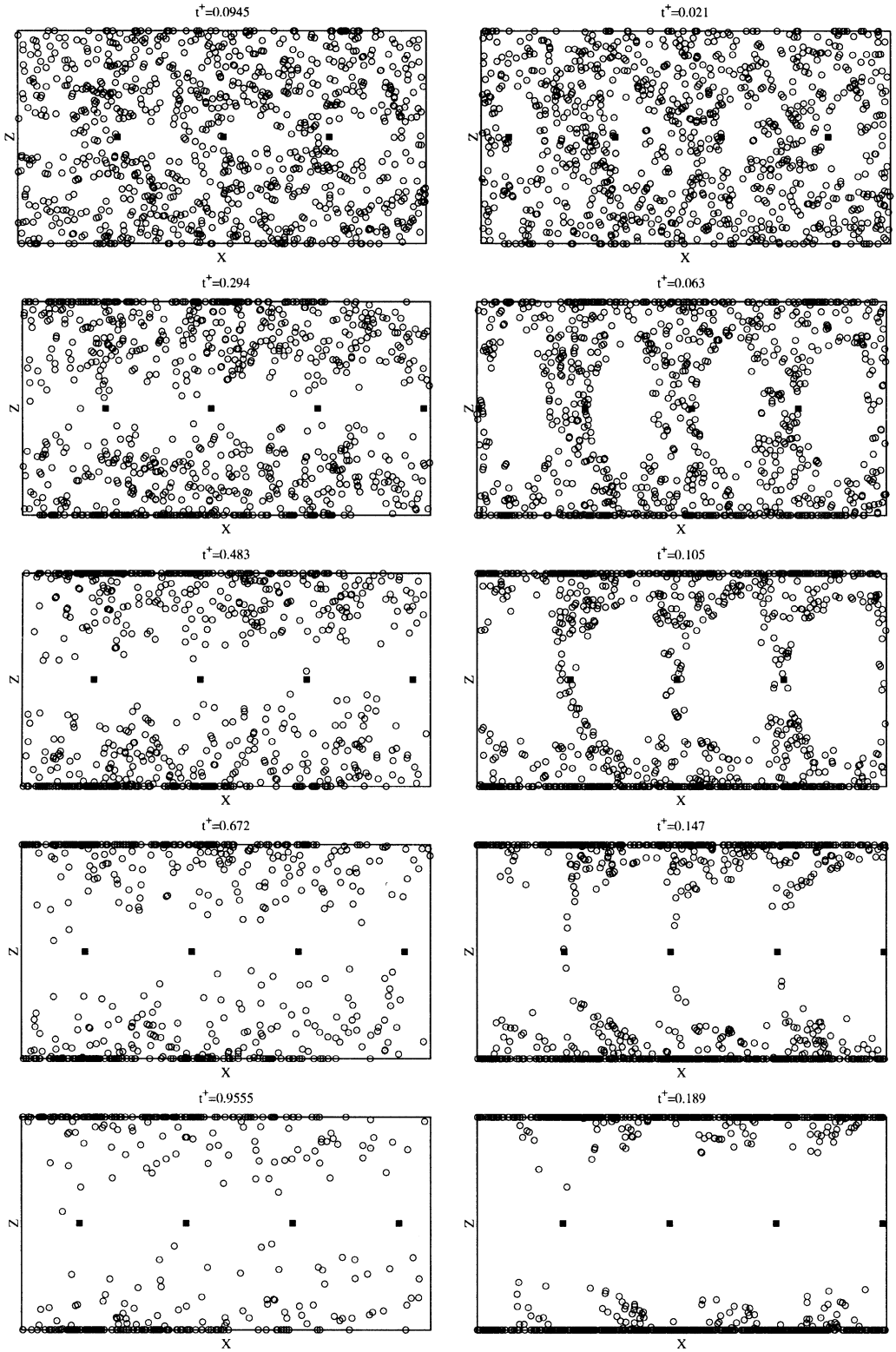

Fig. 3. Dynamics of swarms of 800 particles of different sizes in the high N_{EHD} case. Position of wires is also shown. Snapshots are taken at different simulation times t^+. (Left Side) 4 μm particles; (Right Side) 16 μm particles.

influenced more by their inertia and by the electrostatic force. They appear to lag behind the flow in the central region of the channel, but they travel faster downstream than the fluid in the wall region. We explained before (see Fig. 3) that in the central region of the channel

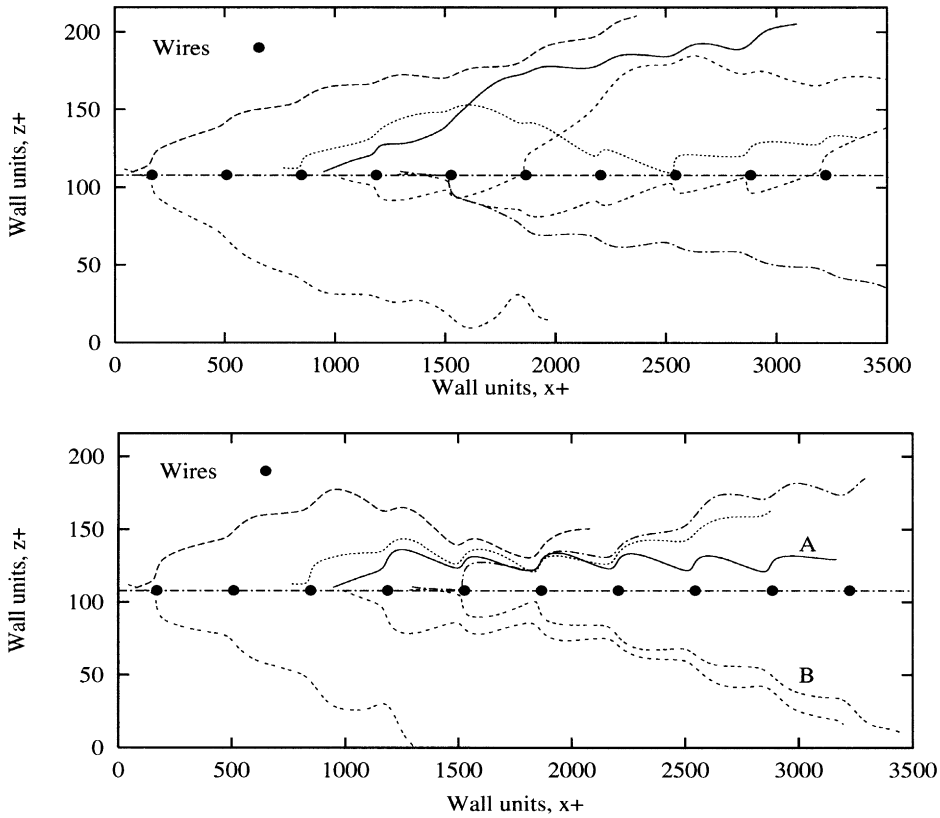

Fig. 4. Examples of trajectories of particles leaving central region of duct in x–z plane. (a) low N_{EHD} case; (b) high N_{EHD} case.

particles are held back by the adverse streamwise component of the electrostatic field. In the wall region, larger particles are likely to travel faster than the fluid because they drift toward the wall from regions at higher fluid streamwise velocity. Since they drift fast and have larger inertia, they do not appear to have enough time to adjust to the local fluid velocity.

3.2. *Effect of EHD flows on particle collection*

One of the aims of this work was to establish whether EHD flows are detrimental for ESP efficiency. In the literature, it is widely claimed that EHD flows constitute a source of turbulence increase and thus reduce the efficiency of the precipitator. We have already shown (Soldati and Banerjee, 1998) that turbulence modifications are strictly dependent on the intensity of the electrostatic field and that turbulence never increases significantly in the center of the channel—where turbulent diffusion mechanisms are more effective—for N_{EHD} in the range of industrial and laboratory applications.

In order to evaluate the influence of the EHD flows on particle collection and on collection efficiency, we performed benchmark simulations in which the electrostatic field acted on particles but had no effect on the fluid, i.e. there were no EHD flows. Particles of different size—4, 8, 16, 32 μm—were tracked in the DNS of our previous work (Soldati *et al.*, 1993). These simulations may be regarded as cases in which particles enter the duct precharged and the voltage applied to the wires is not sufficient to trip the ionic discharge.

In Fig. 6, the influence EHD flows have on the particle deposition point at the wall is shown for different size of particles. The plot indicates the probability a particle has to deposit at a certain axial location and was obtained averaging over all particles depositing and over the axial length corresponding to one precipitator cell—the region from one

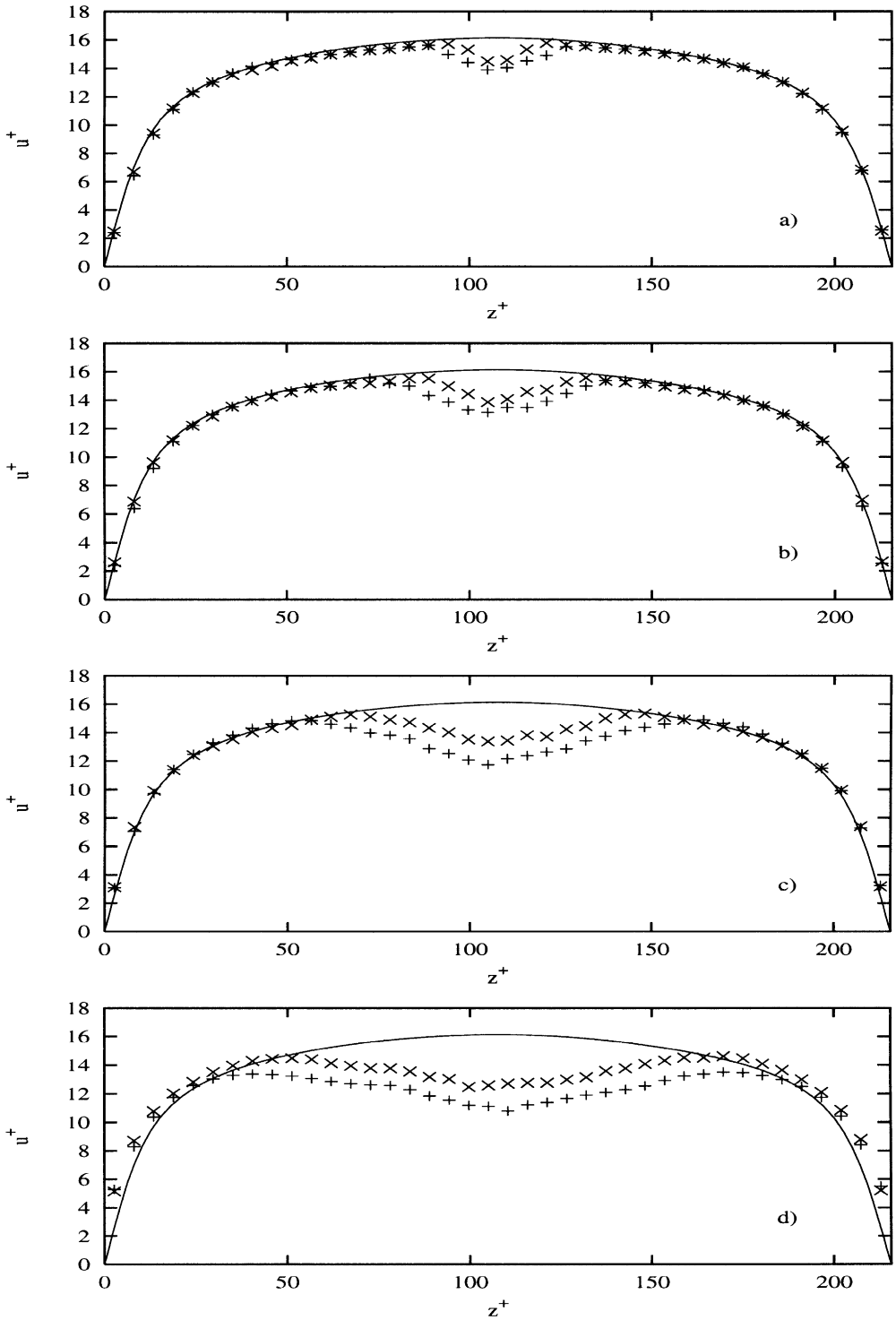

Fig. 5. Mean through velocity of particles calculated averaging over whole computational domain in low N_{EHD} case ($\times$) and in high N_{EHD} case ($+$) compared with that of fluid (continuous line): (a) 4 μm particles; (b) 8 μm particles; (c) 16 μm particles; (d) 32 μm particles.

wire-to-wire midpoint to the next. We consider only the high N_{EHD} case, in which the EHD flows are stronger. It appears that EHD flows have no significant influence on particle deposition point, and also that the probability of the location at which particles deposit is strongly determined by the electric field distribution. Particles tend to have a high

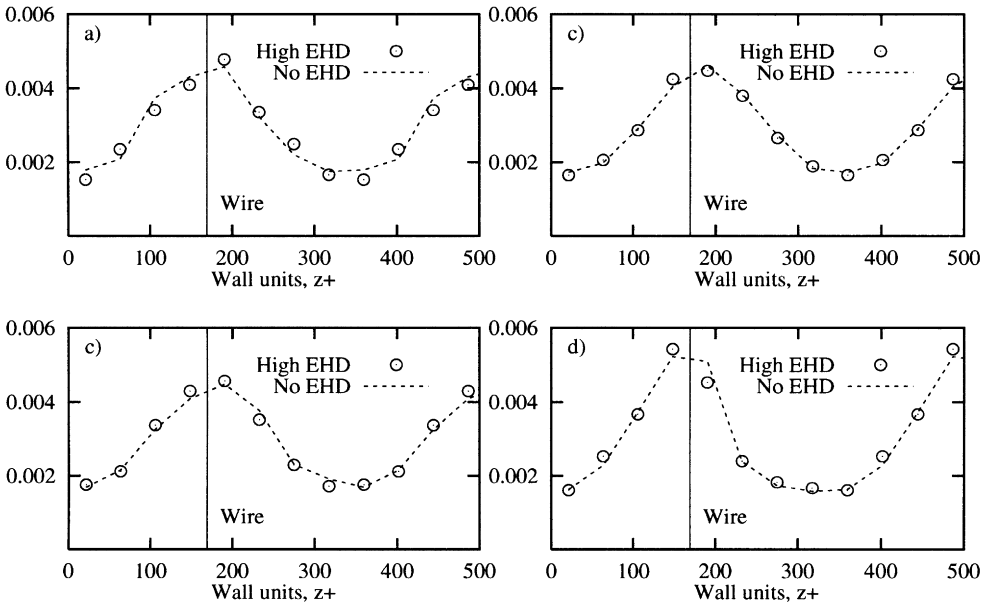

Fig. 6. Influence of EHD flows on probability of particle deposition point in high N_{EHD} case for: (a) 4 μm particles; (b) 8 μm particles; (c) 16 μm particles; (d) 32 μm particles. Probability of particle deposition is normalized by total number of depositing particles. No significant difference is observed due to EHD flows.

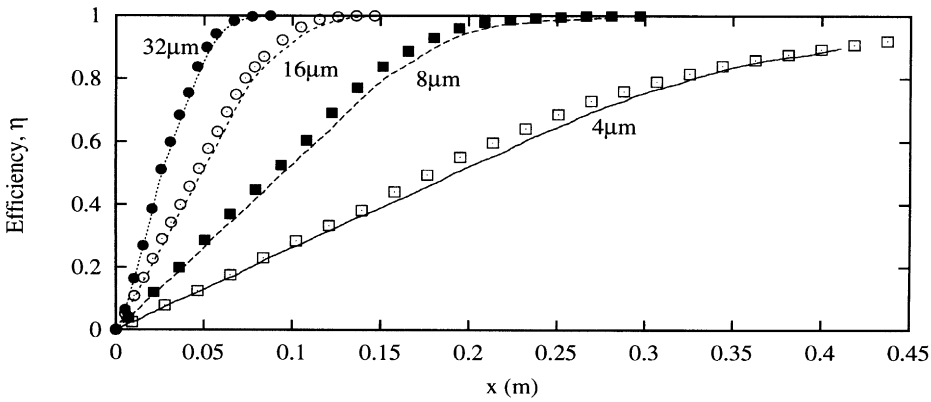

Fig. 7. Effect of EHD flow on overall particle collection. Comparison between high voltage case with EHD flows (lines) and same voltage case with no EHD flows (Symbols) for: (a) 4 μm particles; (b) 8 μm particles; (c) 16 μm particles; (d) 32 μm particles. No significant difference is observed.

probability of depositing slightly downstream the position of the wire, where the electrostatic field is maximum.

However, from Fig. 6d, larger particles—particles with diameter $d_p = 32$ μm—appear to deposit slightly upstream from the wires. The electrostatic body force grows with particle diameter. Thus, we may expect that larger particles start being deflected towards the wall farther upstream from the wire, are then pushed towards the wall stronger than smaller particles and are less likely to be entrained by the streamwise flow.

In Fig. 7, the collection efficiency of the precipitator with EHD flows is compared with that of the precipitator with no EHD flows. The voltage applied in both cases was 42 000 V. It can be observed that efficiency is not affected by the presence of EHD flows. In the case with no EHD effects, the efficiency appears to be somewhat larger. It must, however, be remembered that the mean through flow for the case with EHD flows is slightly larger (6% more) than that of the case with no EHD flows, thus decreasing collection efficiency.

4. CONCLUSIONS AND FUTURE DEVELOPMENTS

The identification of new, better criteria for optimal ESP design requires a thorough understanding of particle transport processes before deposition. In wire-plate ESPs, the turbulent flow field and the presence of EHD flows make theoretical analyses hard and experimental analyses difficult and costly. We used a DNS database to examine the behavior of particles in the flow field resulting from the interaction between EHD flows and the turbulent Poiseuille flow through the precipitator duct. In this way, we were able to determine the influence of EHD flows on particle behavior and on overall collection efficiency.

The first priority of this work was to verify the influence of EHD flows on particles. On examining particle trajectories, it was observed that EHD flows contribute to re-entrain particles in the central region of the channel but also sweep particles toward the wall, thus having a negligible consequence on overall collection efficiency. This was verified by comparing the present simulations with other simulations in which the electrostatic field acted only on particles but not on the fluid. We observed that particle deposition point is scarcely influenced by the presence of EHD flows, rather it is strongly dependent on the distribution of the electrostatic field at the wall. However, we believe that the flow structure at the wall—i.e. turbulence structure interacting with EHD flows—may be crucial to determine the re-entrainment mechanisms of the already deposited particles. Our current research is also focused on this subject.

Direct numerical simulation is, at present, a very expensive tool to be used in practical ESP design. However, this type of simulations can be of help to test new models for particle transport. As a matter of fact, limitations and costs of experimental results and of other numerical techniques have been put in evidence in previous works (Leonard *et al*., 1983; Davidson and McKinney, 1991; Kallio and Stock, 1992; Soldati and Banerjee, 1998).

An industrially acceptable approach for ESP design would be a two-dimensional advection diffusion type equation, as proposed in previous works (Williams and Jackson, 1962; Leonard *et al*., 1982; Soldati *et al*., 1997). The main difficulty with this type of Eulerian model is the *a priori* determination of the transport parameters which are usually tuned onto previous experimental measurements. Current work is aimed at developing *a priori* transport models to be used in a simple advection diffusion equation.

Acknowledgements—The help of Dr. Claudio Alessandro Sisti for performing and analyzing some simulations is greatly appreciated. This work was supported by C.N.R. under Grant No. 95.01146.CT03. Computational resources provided by ENEL/CRT, Pisa, Italy on their CRAY Y-MP2/232 are gratefully acknowledged.

REFERENCES

Atten, P., McCluskey, F. M. J. and Lahjomri, A. C. (1987) The electrohydrodynamic origin of turbulence in electrostatic precipitators. *IEEE Trans. Ind. Appl.* **IA-23,** 705.

Bernstein, S. and Crowe, C. T. (1981) Interaction between electrostatics and fluid dynamics in electrostatic precipitators. *Environ. Int*. **6,** 181.

Brooke, J.W., Kontomaris, K., Hanratty, T. J. and McLaughlin, J.B. (1992) Turbulent deposition and trapping of aerosols at a wall. *Phys. Fluids A* **4,** 825.

Choi, B. S. and Fletcher, C. A. J. (1997) Computation of particle transport in an electrostatic precipitator. *J. Electrostat*. **40&41,** 413.

Choi, B. S. and Fletcher, C. A. J. (1998) Turbulent particle dispersion in an electrostatic precipitator. *Appl. Math. Modell.* **22,** 1009.

Cooperman, P. (1982) Particle transport in electrostatic precipitators—discussion. *Atmospheric Environment* **16,** 1568.

Crowe, C.T., Chung, J.N. and Troutt, T.R. (1988) Particle mixing in free shear flows. *Progr. Energy Comb. Sci.* **14,** 171.

Davidson J. H. and McKinney, P. J. (1991) EHD flow visualization in the wire-plate and barbed plate electrostatic precipitator. *IEEE Trans. Ind. Appl.* **27,** 154.

Deutsch, W. (1922) Bewegung und Ladung der Elektrizititätsträger in Zylinder Kondensator. *Ann. Phys.* **58,** 335.

Gallimberti, I. (1998) Recent advancements in the physical modelling of electrostatic precipitators. *J. Electrostat.* **43,** 219.

Kallio, G. A. and Stock, D. E. (1992) Interaction of electrostatic and fluid dynamic fields in wire-plate electrostatic precipitators. *J. Fluid Mech.* **240,** 133.

Kihm, K. D. (1987) Effects of nonuniformities on particle transport in electrostatic precipitators. Ph.D. diss., Stanford Univ., Stanford, CA.

Koopmans, G. (1988) The electrohydrodynamic origin of turbulence in electrostatic precipitators—Discussion. *IEEE Trans. Ind. Appl.* **IA-24,** 700.
Lai, F. C., McKinney, P. J. and Davidson, J. H. (1995) Oscillatory electrohydrodynamic gas flows. *J. Fluids Eng. ASME Trans.* **117,** 491.
Leonard, G. L., Mitchner, M. and Self, S. A. (1980) Particle transport in electrostatic precipitators. *Atmospheric Environment* **14,** 1289.
Leonard, G. L., Mitchner, M. and Self, S. A. (1982) Experimental study of the effect of turbulent diffusion on precipitator efficiency. *J. Aerosol Sci.* **13,** 271.
Leonard, G. L., Mitchner, M. and Self, S. A. (1983) An experimental study of the electrohydrodynamic flow in electrostatic precipitators. *J. Fluid Mech.* **127,** 123.
Leutert, G. and Bohlen, B. (1972) The spatial trend of electric field strength and space charge density in plate type electrostatic precipitator. *Staub Reinhalt Luft* **32,** 27 (in English).
McDaniel, E.W. and Mason, E.A. (1973) *The Mobility and Diffusion of Ions in Gases.* Wiley, New York.
Pedinotti, S., Mariotti, G. and Banerjee, S. (1992) Direct numerical simulation of particle behavior in the region of turbulent flow in horizontal channels. *Int. J. Multiphase Flow* **18,** 927.
Rowe, P.N. and Henwood, G. A. (1962) Drag forces in hydraulic model of a fluidized bed—Part I. *Trans. Instn. Chem. Engrs.* **39,** 43.
Schmid, H.J. and Umhauer, H. (1996) Investigations on particle dynamics in a plate type electrostatic precipitator using double-pulse holography. *6th Int. Conf. on Electrostatic Precipitation* (*VI ICESP*), Budapest, June 17–22, 1996.
Self, S. A., Mitchner, M. and Kihm, K. D. (1987) Precipitator performance improvement through turbulence control. Proc. *Int. Conf. on Electrostatic Precipitators*, Avano/Venice, Italy, pp. 443–481.
Sisti, C. A. (1997) Lagrangian simulation of turbulent aerosol dispersion in electrostatic precipitators. M.S. thesis, University of Udine, Italy (in Italian).
Soldati, A. (1999) Turbulent dispersion in complex flow fields typical of wire-plate electrostatic precipitators. (In preparation).
Soldati, A., Andreussi, P. and Banerjee, S. (1993) Direct simulation of turbulent particle transport in electrostatic precipitators. *A.I.Ch.E. J.* **39,** 1910.
Soldati, A., Andreussi, P. and Banerjee, S. (1995) Direct simulation of turbulent particle transport in electrostatic recipitators—Reply. *A.I.Ch.E. J.* **41,** 739.
Soldati, A. and Banerjee, S. (1998) Turbulence modification by large-scale organized electrohydrodynamic flows. *Phys. Fluids* **10,** 1742.
Soldati, A., Casal, M., Andreussi, P. and Banerjee, S. (1997) Lagrangian simulation of turbulent particle dispersion in electrostatic precipitators. *A.I.Ch.E. J.* **43,** 1403.
Williams, J. C. and Jackson, R. (1962) The motion of solid particles in an electrostatic precipitator. *Proc. Symp. Interaction Between Fluids and Particles*, *Trans. Inst. Chem. Engrs.* p. 282.
Yeung, P. K. and Pope, S. B. (1988) An algorithm for tracking fluid particles in numerical simulations of homogeneous turbulence. *J. Comp. Phys.* **79,** 373.